EUROFUSION WPPFC-PR(16) 14155

P Stroem et al.

Ion beam analysis of tungsten layers in EUROFER model systems and carbon plasma facing components

Preprint of Paper to be submitted for publication in
Nuclear Instruments and Methods in Physics Research
Section B

This work has been carried out within the framework of the EUROfusion Consortium and has received funding from the Euratom research and training programme 2014-2018 under grant agreement No 633053. The views and opinions expressed herein do not necessarily reflect those of the European Commission.

This document is intended for publication in the open literature. It is made available on the clear understanding that it may not be further circulated and extracts or references may not be published prior to publication of the original when applicable, or without the consent of the Publications Officer, EUROfusion Programme Management Unit, Culham Science Centre, Abingdon, Oxon, OX14 3DB, UK or e-mail Publications.Officer@euro-fusion.org

Enquiries about Copyright and reproduction should be addressed to the Publications Officer, EUROfusion Programme Management Unit, Culham Science Centre, Abingdon, Oxon, OX14 3DB, UK or e-mail Publications.Officer@euro-fusion.org

The contents of this preprint and all other EUROfusion Preprints, Reports and Conference Papers are available to view online free at http://www.euro-fusionscipub.org. This site has full search facilities and e-mail alert options. In the JET specific papers the diagrams contained within the PDFs on this site are hyperlinked

Tungsten Tracing in Wall Materials from Fusion Experiments with MEIS, RBS and ERDA

Petter Ström[1], Per Petersson[1], Anders Hallén[2], Marek Rubel[1], Daniel Primetzhofer[3], Sebastijan Brezinsek[4], Arkadi Kreter[4], Bernhard Unterberg[4], Gennady Sergienko[4], Kazuyoshi Sugiyama[5]

[1]Department of Fusion Plasma Physics, School of Electrical Engineering, KTH Royal Institute of Technology, SE-10044 Stockholm, Sweden

[2]School of Information and Communication Technology, KTH Royal Institute of Technology, SE-10044 Stockholm, Sweden

[3]Department of Physics and Astronomy, Ion Physics, Uppsala University, P.O. Box 516, SE-75120 Uppsala, Sweden

[4]Forschungszentrum Jülich GmbH, Institut für Energie- und Klimaforschung – Plasmaphysik, D-52425 Jülich, Germany

[5]Max-Planck-Institut für Plasmaphysik, D-85748 Garching, Germany

Corresponding author

Petter Ström, pestro@kth.se

Tel. +46 8 790 6111

Abstract

Medium energy ion scattering, Rutherford backscattering spectrometry and elastic recoil detection analysis were used to characterize tungsten layers on plasma-facing components from fusion experiments and related samples in three cases. The tungsten-enriched surface layers in two EUROFER steel-like iron/tungsten test samples, exposed to sputtering by deuterium ions, were measured. Despite very different exposure parameters (in particular a two orders of magnitude difference in ion dose), the total amount of tungsten atoms per unit area in the layers were similar for the two samples ($2 \cdot 10^{15}$ and $3.3 \cdot 10^{15}$ atoms/cm^2 respectively). A depth profile featuring exponential decrease in tungsten content towards higher depths with 10-20 atomic percent of tungsten at the surface and a decay constant between 0.05 and 0.08 Å^{-1} was indicated in one sample, whereas only the total areal density of tungsten atoms was measured in the other. Implanted tungsten layers in a molybdenum mirror were also studied and compared with a simulation based on the implantation parameters. Finally, two different beams, iodine and chlorine, were employed for elastic recoil detection analysis of the deposited layer on a polished graphite plate from a test limiter in the TEXOR tokamak following experiments with tungsten hexafluoride injection. The chlorine beam was preferred for tungsten analysis, mainly because it (as opposed to the iodine beam) does not give rise to problems with overlap of forward scattered beam particles and recoiled tungsten in the spectrum.

Keywords: Fusion, Tungsten, EUROFER, MEIS, ERDA, RBS

PACS: 28.52.Fa, 82.80.Yc

1. Introduction

In tokamak type fusion devices [1], such as the Joint European Torus (JET) and the International Thermonuclear Experimental Reactor (ITER), the latter of which is currently under construction, a hydrogen plasma is magnetically confined within a toroidal vacuum chamber. Plasma-wall interactions (PWIs) occur when energetic particles escape the confinement and impinge on the surrounding first wall. Such interactions lead to erosion of plasma-facing components (PFCs) and subsequent transport of the eroded material in the torus. This material may either end up in the plasma core where it constitutes an unwanted impurity [2], or it may be deposited elsewhere on the wall, possibly together with fuel atoms (deuterium and tritium) [3], forming so called co-deposits. The study of PWIs is multi-disciplinary: it comprises atomic physics, plasma physics and material physics among other fields [4]. The final outcome of the research effort is the design and material selection for the plasma-facing wall. A full metal wall is currently envisioned for ITER. It will feature beryllium for the main chamber and tungsten in the divertor: the part of the machine where heat and particle fluxes are most severe [5]. As a result of this configuration one may expect tungsten erosion and transport in the plasma, followed by deposition on PFCs [6]. Methods to detect small amounts of tungsten on component surfaces are desirable to study such phenomena in current devices, especially JET which began operating with an ITER-like wall in 2009 [7,8]. To provide an overview of the benefits and drawbacks of selected ion beam analysis techniques for tungsten detection on PFCs, we present here three cases where we have measured the tungsten content on fusion-relevant samples with time-of-flight medium energy ion scattering (ToF-MEIS), Rutherford backscattering spectrometry (RBS) and time-of-flight elastic recoil detection analysis (ToF-ERDA).

Abbreviations

ToF: Time-of-flight
ERDA: Elastic recoil detection analysis
MEIS: Medium energy ion scattering
RBS: Rutherford backscattering spectroscopy
PWI: Plasma-wall interaction
PFC: Plasma-facing component
JET: Joint European Torus (fusion experiment in Abingdon, England)
ITER: International Thermonuclear Experimental Reactor (fusion experiment under construction in Cadarache, France)

2. Description of the cases: Methods and Results

2.1 EUROFER steel

Requirements of safety and environmental friendliness related to long-term radioactivity in materials have led to the development of the reduced activation steel EUROFER [9]. It is a prime candidate for use in the first fusion demonstration reactor, DEMO, and later on in power producing commercial machines. In order to achieve low activation under heavy neutron irradiation, regular alloying materials like nickel and molybdenum have been replaced by tungsten and a small amount of tantalum. When the material is exposed to plasma, preferential sputtering [10-12] gives rise to an enrichment of tungsten close to the surface. Knowledge of the characteristics of the enriched layer is essential before the material is included in the design of a fusion reactor. Therefore, in order to study the process of tungsten enrichment, experiments have been performed with sputtering of EUROFER-like iron/tungsten test samples. We have analyzed two different such samples, referred to below as Sample A and Sample B. Both of the test samples were sputtered by deuterium ions, however the details of the treatment were quite different. Table 1 summarizes the composition of the samples before the respective deuterium ion exposure and gives information about the parameters of those exposures. Further information about the machines where the exposures were performed; PSI-2 in Jülich, Germany and the so-called high current ion source in Garching, Germany are given in refs. [13] and [14] respectively.

Table 1: *Original composition of iron/tungsten test samples and deuterium ion exposure parameters. Percentage values for elements in columns 2-3 represent atomic fractions. The projected ranges on row 5 are for single deuterium ions, with the energy from row 4, in Fe by SRIM. Sputtering yields for deuterium with the given energy in Fe and W are taken from the compilation of experimental data and theoretical fits in [15]. For sample A, the yield is evaluated for 75 eV/D.*

Original Composition			**Sputtering parameters**		
Element	**Sample A [%]**	**Sample B [%]**	**Quantity**	**Sample A**	**Sample B**
Fe	98	97	Ion species	D^+	D_3^+
C	0.6	0.07	Energy [eV/D]	50-100	200
W	0.5	1.4	Projected range [Å]	8-12	20
Si	0.5	0.4	Sputtering yield, Fe	$4 \cdot 10^{-3}$	$2.4 \cdot 10^{-2}$
N	0.1	0	Sputtering yield, W	$< 10^{-6}$	$1.5 \cdot 10^{-5}$
O	0.08	1	Dose [D/m^2]	10^{25}	10^{23}
Others (Σ)	< 0.3	< 0.2	Temperature [K]	< 370	570
			Location	PSI-2, Jülich	High current ion source, IPP Garching

Sample A was studied with RBS and the result was compared to that obtained from an unexposed, otherwise identical sample. The analyzing beam, at normal incidence to the sample surface, consisted of 2 MeV ^{4}He. Backscattered particles were detected at 170^o with a solid-state silicon detector whose resolution was 20 keV. In Fig.1, the results are shown with overlays of the best-fitting SIMNRA [16] simulations. For the unexposed sample, the simulated material is simply a mixture of 99.4% iron and 0.6% tungsten. Other elements present in the sample are not discernible in the spectrum since information pertaining to them

is mixed with that of deeper-laying iron at low energies. After deuterium sputtering, the presence of a tungsten-enriched layer at the surface of Sample A is clearly seen, and the best fitting simulation suggests that this layer contains $2 \cdot 10^{15}$ atoms/cm^2 situated on top of an otherwise unchanged bulk.

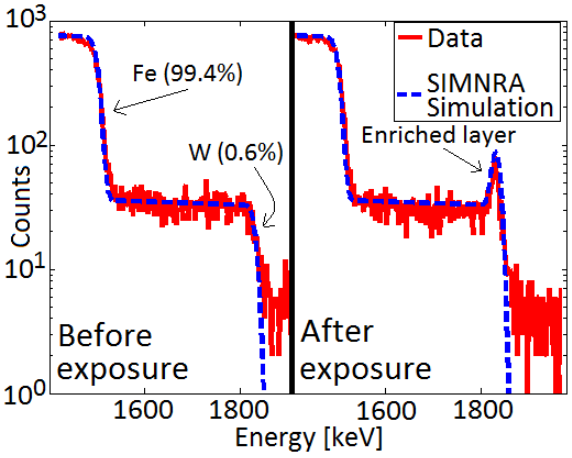

Fig. 1: *RBS spectrum from sample A (right), and an identical sample that was not exposed to deuterium sputtering (left).*

For Sample B, two ToF-MEIS measurements were performed with a ^{4}He beam at 80 keV for normal incidence. In the first measurement, the detector (the full setup is described further in [17]), with an energy resolution of 1.1 keV as found by studying the spectrum from a thin reference Pt film, was placed at 155^o with respect to the forward beam direction (25^o exit angle with respect to the sample normal for outgoing particles) and subsequently it was set to 110^o (70^o exit angle) to further enhance depth resolution. The results are shown by the solid line graphs in Figures 2 (a) and (b). Best fitting simulation results using the TRIM [18] based Monte Carlo code TRBS by J. Biersack and E. Steinbauer are represented by the dashed lines. In these simulations we have taken into account on average ten nuclear collisions events for every backscattered particle track and the outputs were convolved with a 1.1 keV FWHM Gaussian function in order to properly account for the detector resolution. The y-scales in Fig.

2 are those from the simulation, but they are in any case rather arbitrary since they depend upon the total amount of ions hitting the sample, i.e. among other things the irradiation time.

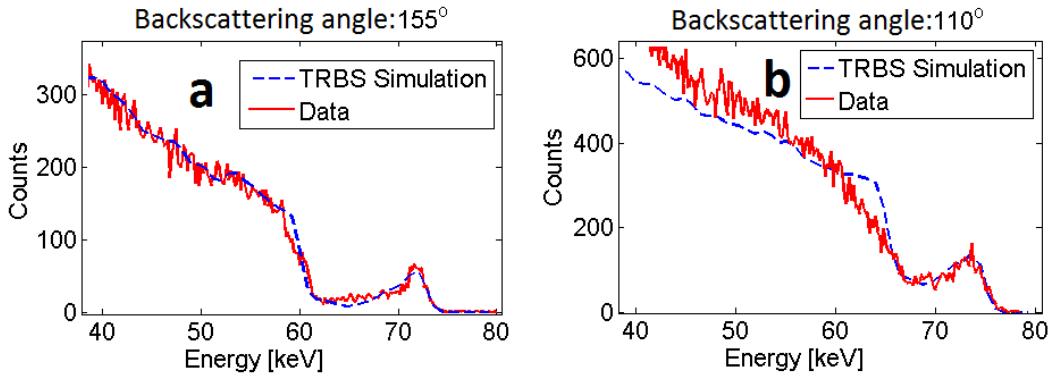

Fig. 2: *MEIS spectra from sample B with best-fitting TRBS simulation at (a) 25° exit angle and (b) 70°.*

The simulation is in agreement with experimental data for the full energy range in Fig. 2 (a). When the exit angle is shallow with respect to the sample surface, however, it becomes hard to fit the lower-energy part of the spectrum as seen in Fig. 2 (b). We do not offer a single explanation for this, but we note that surface roughness of the samples may play a role [19]. Its detrimental effect on the quality of data is expected to become more severe at shallow angles. We do not exclude the possibility of oxide at the sample surface as an explanation for the slight discrepancy between experiment and simulation at the iron edge (between 60 and 70 keV), both in Fig. 2 (a) and (b). The depth profile that gave rise to the simulated spectra in Fig. 2 is shown by the solid line graph in Fig. 3. The total layer thickness as described by this profile corresponds approximately to the projected range of deuterium ions given in table 1. Even though a set of layers in discrete steps is sufficient for a good fit to measured data, we suggest that the actual depth profile displays exponential decay, from a surface level of 10-20 atomic percent W down to the bulk percentage with a decay constant between 0.05 and 0.08 $Å^{-1}$. The dashed curve in Fig. 3 provides an example with 16% W at the surface and a decay

constant of 0.065 $Å^{-1}$. The total W abundance in the simulated layer, down to 70 Å of depth, is $3.3 \cdot 10^{15}$ atoms/cm^2. This number was obtained by considering the atomic density in the simulated layer as the average of iron and tungsten densities, weighted by their respective percentages. It is interesting to note that this abundance is very similar for Samples A and B, even though the exposure parameters were very different – especially the ion dose, which was two orders of magnitude higher for Sample A. We speculate that the reason for this is that the tungsten enriched layer reaches equilibrium after a certain dose, and does not change under continued irradiation (the surface is simply eroded without further change in composition). Given the sputtering yields from Table 1 and using the simple expression 4 from [10] for the equilibrium surface density ratio in a binary alloy, we would in that case expect approximately 20 times more tungsten than iron at the surface of sample B (and an even more extreme ratio in sample A). Obviously this is not the case; however a more realistic model is described in [11]. Taking diffusivity into account, this model also predicts an exponentially decaying tungsten concentration, in accordance with our data.

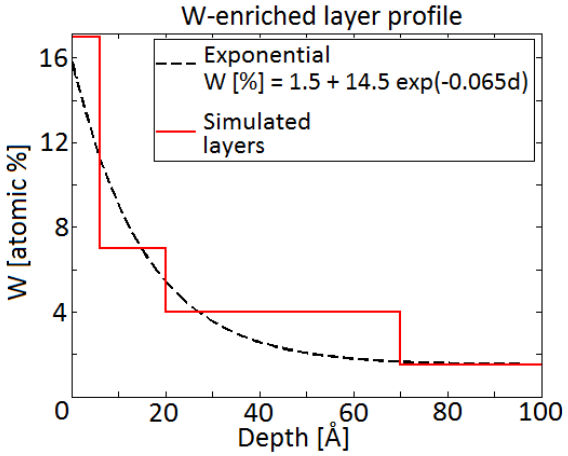

Fig. 3: *Simulated layers in sample B, with an overlain exponentially decaying function suggesting the real layer profile.*

2.2 Diagnostic mirrors

All optical diagnostic systems in ITER will be based on so-called first metal mirrors. Some of these will be in close proximity to the plasma, and as such they are expected to suffer radiation, erosion, deposition and ion implantation [20,21]. Tungsten implantation is of interest in this context, especially for mirrors in and close to the divertor [22]. Experiments in which clean mirrors have been exposed to plasma and subsequently characterized with ERDA and RBS have already been carried out [23,24]. The changes in surface composition have, in these experiments, been related to reflectivity degradation of the mirrors. In the case presented here, we have aimed at studying layers resulting from controlled implantation of tungsten in a molybdenum mirror and comparing to the expected profile as simulated with TRIM. The implantation took place at the implanter facility at the Ion Physics Department of Uppsala University. A 1 cm^2 surface was uniformly bombarded with $1 \cdot 10^{15}$ ^{184}W ions at 40 keV, followed by $1 \cdot 10^{15}$ more at 200 keV. Plots in Fig. 4 (a) show a TRIM simulation of the implantation depth profile, i.e. the amount of tungsten as a function of depth. The implanted mirror was studied by RBS using the same setup as for EUROFER Sample A (see section 2.1). A simplified layer, displayed in Fig. 4 (b) was used as basis for the simulation that is shown together with the measurement result in Fig. 5. Note that the depth scale has been converted between Figures 4 (a) and (b) assuming that 1 atom/cm^2 corresponds to 1.56 Å, as in pure solid molybdenum at room temperature.

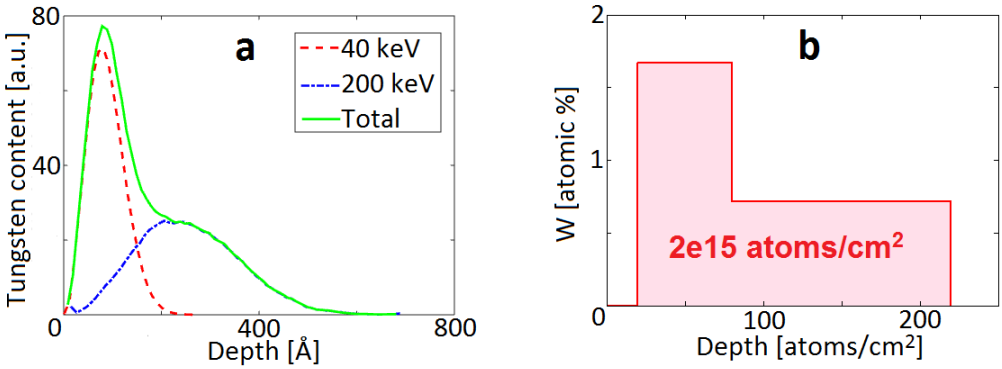

Fig. 4: *(a) TRIM simulation of the ^{184}W depth profile in a clean molybdenum mirror after implantation and (b) simplified profile for SIMNRA simulation.*

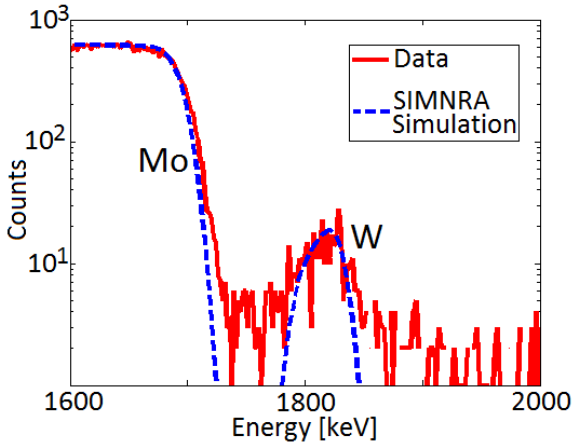

Fig. 5: *RBS spectrum of W-implanted molybdenum mirror with simulation using the simplified layer.*

The good fit to the data that is seen in Fig. 5 is not unique for the simulated layer from Fig. 4 (b). Variations of thickness or tungsten content in the two depth regions on the order of 30% still give a good correspondence to the measurement whereas larger deviations start to show notable changes in the spectrum. Thus, we cannot conclude that the implanted layer is well resolved by RBS here. We conclude however, that the implantation depth profile corresponds to the TRIM simulation within the resolution we obtain with RBS. The total amount of implanted atoms is also consistent. This is a preliminary result and continued work will include studying the relation between the implanted tungsten depth profile and reflectivity degradation in molybdenum mirrors.

2.3 Tungsten transport experiment in the TEXTOR tokamak

In order to gain information about the transport of tungsten in a tokamak plasma, tungsten hexafluoride (WF_6) gas has been injected into discharges during dedicated experiments in the tokamak TEXTOR [25]. That machine was in operation at the Jülich Research Center, Germany, until December 2013. Our third case concerns the so-called test limiter; with a polished graphite plate through which the injection took place. A part of the injected tungsten has been promptly deposited on this plate. It has previously been analyzed by Time-of-Flight ERDA, using iodine as primary beam particles, and nuclear reaction analysis, in order to quantify nitrogen-15 and tungsten [26]. A problem when depth profiling tungsten deposits with heavy ion (e.g. iodine) ERDA is that forward scattered heavy ions and tungsten recoils end up very close to each other in the spectrum, with partial overlap of signals. This fact complicates quantitative analysis. We have performed ToF-ERDA measurements with chlorine and bromine beams to circumvent the problem. These experiments provide similar spectra and thus we focus here on the comparison between using iodine and chlorine only. Fig. 6 (a) shows an iodine ERDA spectrum ($^{127}I^{8+}$, 36 MeV) resulting from addition of the data obtained in seven points scattered over the graphite plate. All elements present on the plate are indicated in the figure. In Fig. 6 (b), the same type of spectrum, but for a 32 MeV $^{35}Cl^{7+}$ beam, is shown. For practical reasons, the points from which data has been gathered are not exactly the same for the two measurements. This fact could explain minor differences in the relative amount of counts for different elements. Apart from that, the first obvious qualitative difference between the two spectra is that the forward scattered iodine counts are mixed with those from tungsten, making it impossible to clearly distinguish relevant information, whereas chlorine is neither interfering with tungsten, nor light elements. The forward scattered chlorine is, in fact, a source of additional information about the tungsten

layer here, since the low stopping power for chlorine in the sample matter as compared to that for tungsten allows a larger information depth than if only the tungsten recoils were to be studied. Furthermore, the high kinematic factor for forward scattered chlorine as compared to recoiled tungsten will, in some cases, give rise to an improvement of depth resolution. The second big difference between the two ToF-ERDA spectra is that a lot of ^{4}He is seen in Fig. 6 (a), but not in (b). This is not due to the different beams used, but rather has to do with the fact that the iodine ERDA measurements were performed shortly after removal of the test limiter from TEXTOR, while the measurement with chlorine beam took place almost two years later. During the intermediate period of storage, helium (not being chemically bound) has most likely desorbed from of the graphite plate. A reduction of hydrogen and deuterium content is also seen due to desorption of water molecules. Further studies of the timescale of helium desorption would be of interest for fusion development, especially if it could also be observed in tungsten or EUROFER samples, both of which suffer property degradation from helium retention [27,28].

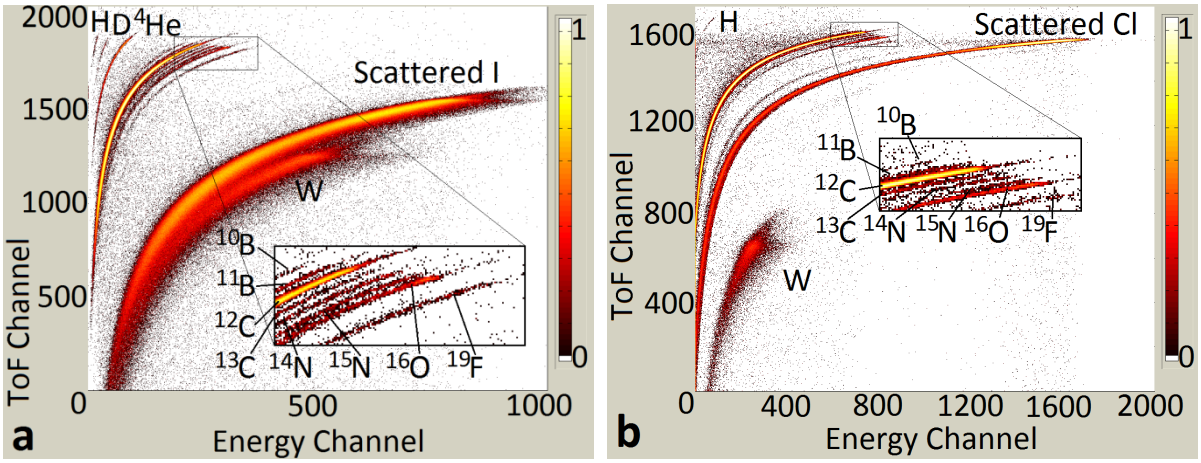

Fig. 6: *Time-of-Flight ERDA spectra on the graphite test limiter from TEXTOR WF_6 experiments with (a) iodine and (b) chlorine beam. Color scale: number of counts in channel relative to maximum number of counts.*

Given the good separation of tungsten counts from those of other elements in Fig. 6 (b), it is clear that probing ions of medium mass, like chlorine, provide a good alternative if tungsten, or other high-Z elements, are to be depth profiled with ToF-ERDA. As previous studies have shown [29], however, care should be taken about surface roughness, especially of carbon samples, which can otherwise easily lead to misinterpretations of measured data. This is particularly troublesome when using shallow angle irradiation methods such as ERDA.

3. Summary with concluding remarks

Through the three cases presented here, we have shown the relevance of ToF-MEIS, RBS and ToF-ERDA for tungsten tracing in fusion reactor wall materials and pointed out a few subjects for possible additional research. Regarding the few nanometer thick W-enriched layer in EUROFER-like iron/tungsten test samples sputtered by deuterium ions; the total amount of tungsten atoms in the layer on Sample A was measured with RBS. Details of the depth profile in Sample B could be resolved with ToF-MEIS. It was noted that, despite a hundred times higher ion dose for Sample A as well as differences in other exposure parameters, both enriched layers contained a few times 10^{15} tungsten atoms. As a consequence, the hypothesis that the enriched layers on both samples have reached equilibrium with respect to preferential sputtering was suggested. From the point of view of fusion, the surface-enrichment of tungsten in EUROFER makes it less vulnerable to sputter erosion. RBS was used to study an implanted tungsten layer in molybdenum with features on the depth scale of tens of nanometers. The depth profile corresponded well to TRIM simulation. This prompted the intention to continue work with determining the relationship between implanted tungsten profiles and reflectivity degradation in molybdenum mirrors. ERDA measurements with iodine and chlorine beams were compared and the differences between the spectra with these two beams were discussed for the case of tungsten-rich

deposited layers on a polished graphite plate from the TEXTOR tokamak. The chlorine beam was preferred due to less interference between counts from forward scattered beam particles and heavy elements from the sample. The loss of almost all retained helium in the plate due to desorption during the period of intermediate storage for two years between the measurements was indicated.

Acknowledgment

We wish to thank Armin Weckmann at KTH, Stockholm and Thomas Schwarz-Selinger at IPP, Garching for help with proof-reading of the article and support during the writing process. This work has been carried out within the framework of the EUROfusion Consortium and has received funding from the European Union's Horizon 2020 research and innovation programme under grant agreement number 633053. The views and opinions expressed herein do not necessarily reflect those of the European Commission.

References

[1] Jardin SC, Bathke CG, Ehst DA, Kaye SM, Kessel Jr CE, Lee BJ et al. Physics Basis for a tokamak fusion power plant. Fusion Eng Des 2000;48:281-98.

[2] Vojtsenya VS, Cohen SA. Scrape-off layer plasma impurities and the choice of candidate materials for the fusion reactor first wall. J Nucl Mater 1990;176-177:611-7.

[3] Federici G, Coad JP, Haasz AA, Janeschitz G, Noda N, Philipps V et al. Critical plasma-wall interaction issues for plasma-facing materials and components in near-term fusion devices. J Nucl Mater 2000;283-287:110-9.

[4] Federici G, Skinner CH, Brooks JN, Coad JP, Grisolia C, Haasz AA et al. Plasma-material interactions in current tokamaks and their implications for next step fusion reactors. Nucl Fusion 2001;41:1967-2110.

[5] Pitts RA, Carpentier S, Escourbiac F, Hirai T, Komarov V, Lisgo S et al. A full tungsten divertor for ITER: Physics issues and design status. J Nucl Mater 2013;438:S48-56.

[6] van Rooij GJ, Coenen JW, Aho-Mantila L, Brezinsek S, Clever M, Dux R et al. Tungsten divertor erosion in all metal devices: Lessons from the ITER like wall at JET. J Nucl Mater 2013;438:S42-7.

[7] Matthews GF, Edwards P, Hirai T, Kear M, Lioure A, Lomas P et al. Overview of the ITER-like wall project. Phys Scr 2007;T128:137-43.

[8] Matthews GF, Beurskens M, Brezinsek S, Groth M, Joffrin E, Loving A et al. JET ITER-like wall - overview and experimental programme. Phys Scr 2011;T145:014001.

[9] Lucon E, Benoit P, Jacquet P, Diegele E, Lässer R, Alamo A et al. The European effort towards the development of a demo structural material: Irradiation behavior of the European reference RAFM steel EUROFER. Fusion Eng Des 2006;81:917-23.

[10] Shimizu H, Ono M, Nakayama K. Quantitative Auger Analysis of Copper-Nickel Alloy Surfaces After Argon Ion Bombardment. Surf Sci 1973;36:817-21.

[11] Ho PS. Effects of Enhanced Diffusion on Preferred Sputtering of Homogeneous Alloy Surfaces. Surf Sci 1978;72:253-63.

[12] Shimizu R. Preferential Sputtering. Nucl Instr Meth Phys Res 1987;B18:486-95.

[13] Reinhart M, Pospieszczyk A, Unterberg B, Brezinsek S, Kreter A, Samm U et al. Using the radiation of hydrogen atoms and molecules to determine electron density and temperature in the linear plasma device PSI-2. Fusion Sci Technol 2013;63:201-4.

[14] Roth J, Bohdansky J, Ottenberger W, Data on Low Energy Light Ion Sputtering: Technical report IPP 9/26, Max-Planck-Institut für Plasmaphysik, Boltzmannstrasse 2, 85748 Garching, Germany, 1979.

[15] Eckstein W, Sputtering Yields. In: Behrisch R, Eckstein W, editors. Topics in Applied Physics 110, Sputtering by Particle Bombardment, Experiments and Computer Calculations from Threshold to MeV Energies. Heidelberg, Germany: Springer-Verlag GmbH; 2007. p. 33-186. doi: 10.1007/978-3-540-44502-9.

[16] Mayer M. SIMNRA, a simulation program for the analysis of NRA, RBS and ERDA. In: Duggan JL, Morgan I, editors. Proceedings of the 15th International Conference on the Application of Accelerators in Research and Industry, AIP Conference Proceedings, vol. 475. Woodbury, New York: American Institute of Physics; 1999. p. 541-4. doi: 10.1063/1.59188.

[17] Linnarsson MK, Hallén A, Åström J, Primetzhofer D, Legendre S, Possnert G. New beam line for time-of-flight medium energy ion scattering with large area position sensitive detector. Rev Sci Instrum 2012;83:095107.

[18] Ziegler JF, Biersack JP, Littmark Y. The stopping and range of ions in solids. 2nd ed. New York: Pergamon; 1996.

[19] Mayer M. Ion beam analysis of rough thin films. Nucl Instr Meth Phys Res 2002;B194:177-86.

[20] Litnovsky A, Wienhold P, Philipps V, Sergienko G, Schmitz O, Kirschner A et al. Diagnostic mirrors for ITER: A material choice and the impact of erosion and deposition on their performance. J Nucl Mater 2007;363-365:1395-402.

[21] Costley AE, Sugie T, Vayakis G, Walker CI. Technological challenges of ITER diagnostics. Fusion Eng Des 2005;74:109-19.

[22] Litnovsky A, Voitsenya VS, Costley A, Donné AJH. First mirrors for diagnostic systems of ITER. Nucl Fusion 2007;47:833-8.

[23] Ivanova D, Rubel M, Widdowson A, Petersson P, Likonen J, Marot L et al. An overview of the comprehensive First Mirror Test in JET with ITER-like wall. Phys Scr 2014;T159:014011.

[24] Rubel M, Ivanova D, Coad JP, De Temmerman G, Likonen J, Marot L et al. Overview of the second stage in the comprehensive mirrors test in JET. Phys Scr 2011;T145:014070.

[25] Rubel M, Coenen J, Ivanova D, Möller S, Petersson P, Brezinsek S et al. Tungsten migration studies by controlled injection of volatile compounds. J Nucl Mater 2013;438:S170-4.

[26] Petersson P, Rubel M, Possnert G, Brezinsek S, Kreter A, Möller S et al. Overiew of nitrogen-15 application as a tracer gas for material migration and retention studies in tokamaks. Phys Scr 2014;T159:014042.

[27] Zenobia SJ, Kulcinski GL. Formation and retention of surface pores in helium-implanted nano-grain tungsten for fusion reactor first-wall materials and divertor plates. Phys Scr 2009;T138:014049.

[28] Wang P, Nobuta Y, Hino T, Yamauchi Y, Chen L, Xu Z et al. Helium Retention and Desorption Behaviour of Reduced Activation Ferritic/Martensitic Steel. Plasma Sci Technol 2009;11:226-30.

[29] Ström P, Petersson P, Rubel M, Weckmann A, Brezinsek S, Kreter A, Möller S, Rozniatowski K. Characterisation of surface layers formed on plasma-facing components in controlled fusion devices: Role of heavy-ion elastic recoil detection. Vacuum 2015 [In press, Corrected Proof]. http://dx.doi.org/10.1016/j.vacuum.2015.04.019.